HYDRODYNAMIC CHARACTERISTICS OF TURBULENT FLOW OF AN INCOMPRESSIBLE FLUID IN A CHANNEL WITH POROUS WALLS

V. V. Dil'man, L. I. Krupnik,
and R. Z. Adinberg

UDC 532.5.071.4

The effect of a transverse mass flux and a pressure gradient on the shaping of the flow structure in a channel with porous walls is investigated.

The presence of a transverse mass flux in the boundary layer at a porous surface has a pronounced effect on momentum, heat, and mass transfer [1-6].

Investigations of the structure of flows with suction (blowing) of material in external [1, 3, 5, 7] and internal [2, 6, 9] problems based on integral methods [7, 10] or on various concepts of turbulent viscosity [2-4, 8, 11], together with the available experimental data [6, 9-12], encompass only the region of small transverse mass fluxes $v_w/\bar{u} = 0.001$-0.01 under negligibly small longitudinal pressure gradients. In addition, in various technical fields turbulent flows occur with large values of $v_w/\bar{u}$ and a large positive pressure gradient.

The present study of the structure of turbulent air flow was performed for transverse mass fluxes $v_w/\bar{u}$ from 0.001 to 0.1 and a positive longitudinal pressure gradient dp/dx up to 10^3 $(N/m^2)\cdot m$.

The local values of the longitudinal velocity u and the static pressure p were measured at various cross sections of a cylindrical channel with porous walls and a dead end. The channel had a diameter D = 2R = 70 mm, a length L = 840 mm, and the total area of the 4-mm-diameter holes (d) in the wall comprised 14% of the lateral surface.

The flow was stabilized hydrodynamically by a section of tube 40 diameters long.

The pressure was measured with a pitot head meter having a tube 1 mm in outside diameter and a 0.5-mm inlet. The measuring tube was placed in the stream parallel to the channel axis and displaced radially over the range $0 < r/R < 0.95$. Since under the experimental conditions the downwash angle did not exceed 10°, the curvature of the flow lines did not introduce an error into the measurement of the dynamic pressure [13]. Static pressures were sampled from the wall of a tube having holes 0.5 mm in diameter.* The measurements were performed for a range of Reynolds numbers at the inlet to the test section $Re = 4\cdot10^4$-$1.5\cdot10^5$.

A distinctive feature of fluid flows with a transverse mass flux in a channel with a dead end is a spontaneous and generally nonuniform distribution of radial velocity along the length of the channel [14].

The radial velocity and the nature of its distribution are unknown and independent variables of the problem under consideration and play a decisive role in shaping the quantitative and qualitative laws of flow as a whole. The values of the radial velocity v were determined from the measured profile of the longitudinal velocity by using the equation of continuity

$$\frac{\partial}{\partial x}(ru) + \frac{\partial}{\partial r}(rv) = 0, \tag{1}$$

which, when integrated over the radius of the channel from 0 to r, gives

*From our static pressure measurements at the tube wall and on the axis $\partial p/\partial r = 0$.

Translated from Inzhenerno-Fizicheskii Zhurnal, Vol. 32, No. 4, pp. 588-593, April, 1977. Original article submitted March 30, 1976.

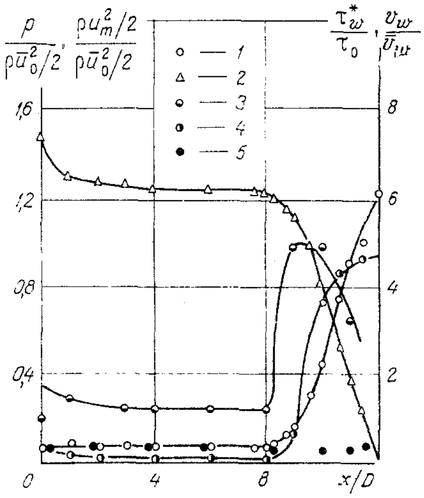
Fig. 1

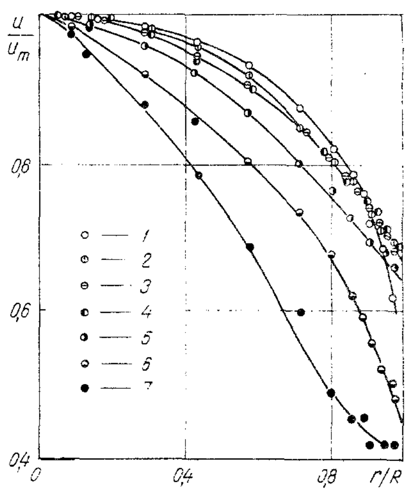
Fig. 2

Fig. 1. Longitudinal variation of the main hydrodynamic flow characteristics in a channel with porous walls (Re_0 = 68,000); 1, 5) $p/(\rho\bar{u}_0^2/2)$; 2) $(\rho u_m^2/2)/\rho\bar{u}_0^2/2)$; 3) τ_w^*/τ_0; 4) $v_w/\bar{v}_w$; 1–4) channel with dead end; 5) channel without dead end.

Fig. 2. Profiles of longitudinal velocity in a channel with porous walls: 1) x/D = 0; 2) 4; 3) 6; 4) 8; 5) 10; 6) 11; 7) 11.5.

$$v = -\frac{1}{r} \cdot \frac{\partial}{\partial x} \int_0^r urdr. \tag{2}$$

For r = R we have

$$v_w = -\frac{R}{2} \cdot \frac{d\bar{u}}{dx}. \tag{3}$$

The results of solving Eqs. (2) and (3) numerically are shown in Fig. 1.

The curve for the distribution of radial velocity at the wall with distance along the channel clearly shows that there are two qualitatively different parts of the motion, in each of which the radial velocity v_w varies monotonically. The first part for x/D < 8 is characterized by a small transverse mass flux varying from $v_w/\bar{u}$ = 0.001 to 0.005; in the second part the radial velocity increases sharply: for x/D = 11.5, $v_w/\bar{u}$ = 0.1, while for x/D = 12, $v_w/\bar{u} = \infty$.

The pressure in the stream is shaped by competing factors. The change in momentum due to suction increases the pressure in the direction of flow, while internal friction leads to energy dissipation. The resultant effect of these factors in the region 0 < x/D < 8 with a very small transverse mass flux leads to a zero pressure gradient dp/dx = 0. It is characteristic that in the absence of a dead end, other conditions being equal, there is a zero pressure gradient over the whole length of the porous wall channel investigated (Fig. 1). Thus the presence of a dead end causes a radical change in the nature of the motion.

The velocity field of the developed turbulent flow in a channel with porous walls is continuously deformed (Fig. 2). For x/D < 8 this leads to a filling in of the profile and an increase in the velocity gradient at the wall. This result agrees with other measurements [3, 9-11]. For gradient flow (dp/dx > 0) with suction the velocity field is peaked, and in the boundary-layer region of the profile the gently sloping portion formed is characteristic of flows with a positive pressure gradient [1] and increases with increasing transverse mass flux [10].

According to the equation of continuity the transformation of longitudinal velocity fields in a cylindrical channel leads to the extremal character of the radial velocity distribution curves (Fig. 3). Taking account of the negative value of the longitudinal velocity gradient for suction (du/dx < 0) we find from Eq. (1) dv/dr > 0 in the flow core. At the channel wall where r = R, v = v_w, and u_w = 0

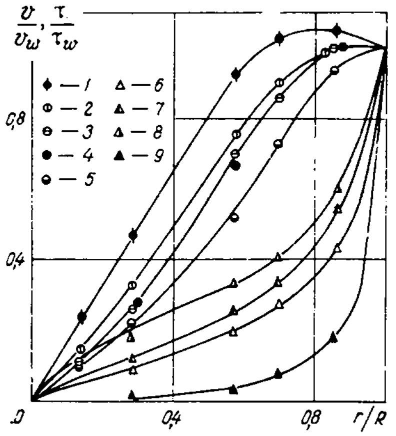

Fig. 3

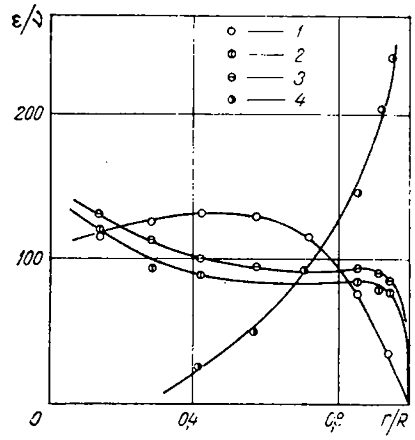

Fig. 4

Fig. 3. Profiles of radial velocity and shear stress: 1-5) v/v_w; 6-9) τ/τ_w^*; 1, 6) x/D = 2; 2, 7) 4; 3) 6; 4, 8) 8; 5) 11; 9) 10.

Fig. 4. Distribution of the coefficient of turbulent viscosity over the channel cross section: 1) x/D = 0; 2) 4; 3) 6; 4) 10.

$$\left(\frac{\partial v}{\partial r}\right)_w = -\frac{v_w}{R},$$

or

$$\left[\frac{\partial (v/v_w)}{\partial (r/R)}\right]_w = \mathrm{tg}\,\alpha = -1. \tag{4}$$

Thus, according to Eq. (4), the normalized radial velocity gradient at the wall is independent of the longitudinal coordinate. Moreover, the analysis of the experimental data (Fig. 3) and the results of other studies [6, 15] shows that

$$\mathrm{tg}\,\alpha = f\left(\frac{x}{D}\right). \tag{5}$$

This implies that $u_w \neq 0$; i.e., the flow lines do not enter the holes in the porous wall normal to the surface, but at a certain angle, as was determined visually in experiments [16, 17].

We write down the equations of motion for the steady axisymmetric turbulent flow of an incompressible fluid [18]:

$$\rho u \frac{\partial u}{\partial x} + \rho v \frac{\partial u}{\partial r} = \frac{\partial \sigma}{\partial x} - \frac{1}{r} \cdot \frac{\partial (\tau r)}{\partial r}, \tag{6}$$

where

$$\sigma = -p + 2\mu \frac{\partial u}{\partial x} - \rho \overline{u'^2}, \tag{7}$$

$$\tau = -\mu\left(\frac{\partial v}{\partial x} + \frac{\partial u}{\partial r}\right) + \rho \overline{u'v'}. \tag{8}$$

Integrating Eq. (6) along the radius of the channel from 0 to r, and using Eqs. (1) and (7), we obtain

$$\tau = -\frac{1}{r} \cdot \frac{\partial}{\partial x} \int_0^r \rho u^2 r dr - \frac{r}{2} \cdot \frac{dp}{dx} - \frac{1}{r} \cdot \frac{\partial}{\partial x} \int_0^r \rho \overline{u'^2} r dr - 2\mu \frac{\partial u}{\partial x} - \rho u v. \tag{9}$$

At r = R, $v = v_w$, $u = u_w$, and $\tau = \tau_w$, Eq. (9) takes the form

$$\tau_w = -\frac{1}{R}\cdot\frac{\partial}{\partial x}\int_0^R \rho u^2 r dr - \frac{R}{2}\cdot\frac{dp}{dx} - \frac{1}{R}\cdot\frac{\partial}{\partial x}\int_0^R \rho\overline{u'^2} r dr - 2\mu\frac{\partial u_w}{\partial x} - \rho v_w u_w. \quad (10)$$

The quantity $\rho v_w u_w$ represents the momentum transferred through the porous wall. The presence of this factor results from the reaction of the separating mass, and affects the value of the pressure gradient in the channel [19].

The premise $u_w = 0$, very common in the literature [2, 6, 12, 14, 15], can lead to an incorrect result for the wall shear stress τ_w. It is easy to see (10) that the value obtained in this way represents the combined effect of dissipation and transverse momentum transfer, and can be thought of as a certain effective value of the shear stress†

$$\tau_w^* = \tau_w + \rho v_w u_w + 2\mu\frac{\partial u_w}{\partial x}. \quad (11)$$

The individual components contribute to the shaping of τ_w^* (Fig. 1) in the following way. For $0 < x/D < 10$, independently of the variation of the flow parameters τ_w and u_w at the wall, the behavior of the curves for $(\tau_w^*/\tau_0)(x/D)$ and $(v_w/\bar{v}_w)(x/D)$ indicates that the suction velocity v_w exerts a dominating effect on τ_w^*. Outside this range the flow structure undergoes qualitative changes: points of inflection appear on the pressure distribution curves and on the longitudinal velocity profile, characteristic of unstable flows [20]. It is possible that close to the dead end where $x/D > 10$, secondary currents arise at the porous wall with a negative value of the longitudinal velocity u_w. According to Eq. (11) this leads to a decrease in the effective shear stress τ_w^*, as is confirmed experimentally (Fig. 1).

The variation of the shear stress over the cross section of a channel with porous walls shown in Fig. 3 differs from the usual linear distribution characteristic of flow in a tube with impenetrable walls. As the transverse mass flux increases, the local values of τ/τ_w^* decrease. This result agrees qualitatively with data in [11]. The observed trend for $v_w/\bar{u} > 0.05$ leads to degeneracy of the turbulent component of the shear stress in the flow core.

The turbulent viscosity can be determined from data on velocity fields and shear stresses by using the equation [18]

$$\frac{\varepsilon}{\nu} = \frac{\tau}{-\mu\left(\frac{\partial v}{\partial x} + \frac{\partial u}{\partial r}\right)} - 1. \quad (12)$$

In the flow core the directed radial current decreases the turbulence of the developed turbulent flow, and in the boundary-layer region where, as a consequence of the discreteness of the suction, the flow lines are considerably deformed, the separation of mass is accompanied by vortex formation (Fig. 4). For a large transverse mass flux this mechanism leads to a laminarization of the flow core and to appreciable turbulence of the boundary-layer region.

NOTATION

p, static pressure; ρ, density; μ, ν, dynamic and kinematic viscosities; u, v, longitudinal and radial velocity components; u', v', fluctuating components of longitudinal and radial velocities; τ, σ, shear and normal stresses; D = 2R, channel diameter; L, channel length; d, diameter of holes in porous wall; Re, Reynolds number; x, r, longitudinal and radial coordinates. Indices: 0, flow parameters at inlet to test section; w, porous wall; m, tube axis. A bar over a quantity denotes its average.

LITERATURE CITED

1. S. S. Kutateladze and A. I. Leont'ev, Heat and Mass Transfer and Friction in a Turbulent Boundary Layer [in Russian], Énergiya, Moscow (1972).
2. R. B. Kinney and E. M. Sparrow, Trans. ASME, Ser. C, 92, 117 (1970).
3. T. Sebesi, Raketn. Tekh. Kosmonavt., 8, No. 12, 15 (1970).
4. S. V. Patankar and D. B. Spalding, Heat and Mass Transfer in Boundary Layers, Morgan-Grampian, London (1967).

†In calculating τ and τ_w from Eqs. (9) and (10) the turbulent normal stress $\rho\overline{u'^2}$ was neglected as a quantity of second order [12].

5. W. M. Kays, Intern. J. Heat Mass Transfer, 15, 1023 (1972).
6. R. M. Olson and E. R. Eckert, Trans. ASME, Ser. E, 88, 7 (1966).
7. S. C. Lubard and F. L. Fernandez, Trans. ASME, Ser. E, 93, 688 (1971).
8. L. Merkin, A. Solan, and Yu. Vinograd, Teploredacha, 93, No. 2, 108 (1971).
9. J. K. Aggarwal, M. A. Hollingsworth, and Y. R. Mayhew, Intern. J. Heat Mass Transfer, 15, No. 9, 1585 (1972).
10. M. O. Frankfurt, in: Industrial Aerodynamics [in Russian], No. 30, Mashinostroenie, Moscow (1973), p. 34.
11. Y. Y. Chan, Trans. CASI, 4, No. 2, 108 (1971).
12. M. Élena, in: Heat and Mass Transfer [in Russian], Vol. 9, Part 2, Minsk (1972), p. 104.
13. S. M. Gorlin and I. I. Slezinger, Wind Tunnels and Their Instrumentation, Israel Program for Scientific Translations, Jerusalem (1966).
14. V. V. Dil'man, S. P. Sergeev, and V. S. Genkin, Teor. Osn. Khim. Tekhnol., 5, 564 (1971).
15. I. I. Paleev, F. A. Arafonova, and L. N. Dymant, Inzh.-Fiz. Zh., 19, No. 3, 406 (1970).
16. V. N. Taliev, Aerodynamics of Ventilation [in Russian], Stroiizdat, Moscow (1954).
17. V. I. Khanzhonkov, in: Industrial Aerodynamics [in Russian], No. 15, Oborongiz, Moscow (1959), p. 5.
18. H. Schlichting, Boundary Layer Theory, McGraw-Hill, New York (1968).
19. G. A. Petrov, Motion of a Fluid with a Variable Flow Rate along Its Path [in Russian], Stroiizdat, Moscow—Leningrad (1951).
20. P. Cheng, Separated Flows [Russian translation], Vol. 1, Mir, Moscow (1972).

ATTACHMENT TO THE IKS-21 SPECTROPHOTOMETER FOR MEASURING THE ANGULAR CHARACTERISTICS OF DIFFUSELY SCATTERING MATERIALS SUBJECT TO HEMISPHEREICAL IRRADIATION

S. G. Il'yasov, V. V. Krasnikov,
E. P. Tyurev, and I. S. Ageenko

UDC 536.3

An attachment to the standard-manufacture IKS-21 spectrophotometer is described; it is designed for measuring the spectral and integrated reflecting powers of diffusely reflecting materials in relation to the angle of observation for the case of hemispherical irradiation in an integrated flow of long- and short-wave infrared radiation.

Data relating to the spectral and integrated characteristics of diffusely reflecting materials subjected to diffuse irradiation in a flow of long- and short-wave infrared radiation, expressed as functions of the angle of observation, are essential for calculating the radiation fields in various materials, for spectral analysis, and for selecting generators to be used in various irradiating infrared installations and furnaces. For thermal engineers' calculations of thermal-radiation installations it is also essential to possess information regarding the hemispherical characteristics $R_\lambda(2\pi)$ and $T_\lambda(2\pi)$ of the materials under consideration under various irradiation conditions. These characteristics are usually measured by methods based on a specular hemisphere of integrating sphere [1-9, 11]. These devices differ from one another as regards the conditions of irradiating the sample and also the means of obtaining the diffuse flow of radiation. The main disadvantage of the majority of such instruments is the limited spectral range of measurements (0.25-3.0 μ). The use of a special integrating sphere [4] enables us to extend the range of the spectrum to 15 μ, but the preparation of such spheres is extremely troublesome. The device mentioned in [5] enables us to

Moscow Technological Institute of the Food Industry. Translated from Inzhenerno-Fizicheskii Zhurnal, Vol. 32, No. 4, pp. 594-601, April, 1977. Original article submitted March 26, 1976.